Machine Learning-Based Noise Spectrum Characterization in a Qutrit System

Angelo Zampronio

October 2025

Abstract

Quantum computing has emerged as a promising technology capable of solving specific computational problems more efficiently than classical approaches. However, a major limiting factor remains: environmental noise acting on qubits . Qubits are extremely sensitive to noise, and understanding its spectral characteristics is fundamental for both modeling its detrimental effects and developing strategies for mitigation . Most studies address noise coupling to two-level systems, yet many physical implementations of qubits originate from multilevel systems truncated to two levels . In this work, we extend noise characterization to qutrit systems, exploring how environmental noise spectra can be identified in a three-level quantum system. Analytical treatment of noise is generally infeasible, as it results from highly complex and system-dependent dynamics that vary across quantum devices . To address this challenge, we propose a machine learning-based approach for extracting the noise spectrum of a qutrit coupled to an arbitrary environment. Through simulations, we demonstrate that the noise spectral density can be inferred from a sequence of specifically designed control pulses followed by fidelity measurements of the system's evolution. This framework provides a general, adaptable method for characterizing noise in multilevel quantum systems.

1 Introduction

The emergence of quantum computers promises advances across multiple scientific and technological domains, including chemistry, materials science, medicine, and cryptography [1, 2, 3, 4, 5, 6]. By exploiting inherently quantum phenomena such as superposition and entanglement, quantum devices can outperform classical computers in solving certain classes of problems.

Despite these prospects, quantum computing is still in the Noisy Intermediate-Scale Quantum (NISQ) era [7]. Current devices, while featuring hundreds of qubits—such as those developed by IBM, Quantinuum, and Microsoft [8, 9, 10]remain noisy and of limited size, preventing fault-tolerant operation and large-scale computations. Consequently, realizing quantum advantage [11] remains an ongoing challenge.

Error accumulation is one of the primary obstacles to scalable quantum computation. As qubits interact with their surrounding environment, unwanted couplings induce decoherence and noise, rapidly degrading the fidelity of quantum operations. Understanding the spectral properties of environmental noise is therefore essential for designing error mitigation protocols and improving qubit coherence times.

While most studies focus on two-level systems [12], real-world qubits are often derived from multilevel quantum systems truncated to two states, such as Transmoms [13]. In such cases, leakage to higher levels represents an additional source of decoherence, the so called leakage [14, 15, 16]. To better capture this behavior, we investigate how the environmental noise spectrum can be characterized in a qutrit system. Understanding the spectrum of noise acting on a qubit can yield valuable information about its environment, and crucially underpins the optimization of dynamical decoupling protocols that can mitigate such noise[17, 18, 19, 20].

In this work, we propose a neural network-based method [21] for identifying static noise spectra in qutrits. Because environmental noise is inherently random and depends on the specific qubit architecture, analytical or system-specific approaches are often impractical. Our method offers a general, data-driven framework capable of learning noise characteristics from simulated or experimental fidelity measurements, paving the way for more accurate modeling and control of multilevel quantum devices. In future work, we expect to extend this approach on not static noise.

2 Proposed Methodology

2.1 Hamiltonian Model

We consider the total Hamiltonian H_T of a qutrit system (comprising states $|0\rangle, |1\rangle, |2\rangle$). H_T can be decomposed as:

$$H_T = H_0 + H_{int} + H_P$$

where $H_0 = \sum_{i=1}^{2} \omega_i |i\rangle\langle i|$ represents the free drift Hamiltonian with transition frequencies ω_i, H_P is the applied control pulse Hamiltonian, and H_{int} is the undesirable interaction with the environment, which constitutes the noise we aim to characterize. In this paper, we are gonna let the qutrit evolve freely, and so $H_G = I$.

The noise interaction H_{int} can be generally expressed in the $SU(3)$ basis using the Gell-Mann matrices λ_i:

$$H_{int} = \sum_{i=1}^{8} c_i(t)\lambda_i \approx \sum_{i=1}^{8} c_i\lambda_i$$

where,

$$\lambda_0 = \begin{pmatrix} 0 & 1 & 0 \\ 1 & 0 & 0 \\ 0 & 0 & 0 \end{pmatrix}, \quad \lambda_1 = \begin{pmatrix} 0 & -i & 0 \\ i & 0 & 0 \\ 0 & 0 & 0 \end{pmatrix}, \quad \lambda_2 = \begin{pmatrix} 1 & 0 & 0 \\ 0 & -1 & 0 \\ 0 & 0 & 0 \end{pmatrix},$$

$$\lambda_3 = \begin{pmatrix} 0 & 0 & 1 \\ 0 & 0 & 0 \\ 1 & 0 & 0 \end{pmatrix}, \quad \lambda_4 = \begin{pmatrix} 0 & 0 & -i \\ 0 & 0 & 0 \\ i & 0 & 0 \end{pmatrix}, \quad \lambda_5 = \begin{pmatrix} 0 & 0 & 0 \\ 0 & 0 & 1 \\ 0 & 1 & 0 \end{pmatrix},$$

$$\lambda_6 = \begin{pmatrix} 0 & 0 & 0 \\ 0 & 0 & -i \\ 0 & i & 0 \end{pmatrix}, \quad \lambda_7 = \frac{1}{\sqrt{3}} \begin{pmatrix} 1 & 0 & 0 \\ 0 & 1 & 0 \\ 0 & 0 & -2 \end{pmatrix}.$$

We adopt two key approximations. First, we assume a stationary (static) noise environment, where the coefficients are constant over the gate time, i.e., $c_i(t) \approx c_i$. This is a common approximation for gate operations that are sufficiently fast. Second, based on the physics of transmon systems, we neglect noise channels that are considered negligible, such as λ_3 and λ_4, they are responsible for transitions between states $|0\rangle$ and $|2\rangle$, small oscillations can effect transitions between neighbor states, but aren't strong enough otherwise,

The order of magnitude of H_0 and H_P will be GHz (10^9).For the intensity of noise, we set it to be 100 times smaller then the pulses, which configures a extreme case of highly noise environment, must of them are in the order of KHz to 1MHz [22, 23].

The evolution of the system over a time τ is thus governed by the unitary operator $U(\tau) = \exp(-iH_T\tau/\hbar)$. Our objective is to predict all c_i so that the evolution operator predicted by the NN is sufficiently equal to the real noise one, in the time-scale of importance. Quantum computers using transmoms are considered very

fast, with one and two qubits gates being faster then 50ns [24, 25]. In some architectures, gates has CNOT are slower, with times of 300ns [26]. In this paper, we will consider the cases of $\tau = 50$ns and $\tau = 300$ns.

2.2 The Qutrit Model and Leakage

The primary motivation for this qutrit approach is the physics of superconducting qubits, particularly the Transmon. The Transmon is a nonlinear oscillator, typically truncated to its two lowest levels to operate as a qubit. This design uses small anharmonicity to make the qubit insensitive to noise, but this simultaneously introduces the risk of **leakage**: an unwanted transfer of population outside the computational subspace (e.g., from $|1\rangle$ to $|2\rangle$). This leakage acts as a significant source of noise, often overlooked in simpler two-level models.

2.3 Pulse-Based Feature Engineering

For each of the six noise coefficients c_k we aim to identify (e.g., $k \in \{0, 1, 2, 4, 5, 6, 7\}$), we apply a set of 10 distinct control pulses. The pulse Hamiltonian takes the form:

$$H_P^{(k,n)} = n\omega_0\lambda_k$$

where n is an integer strength parameter, $n \in \{0, 1, ..., 9\}$. The total Hamiltonian for a given experiment (k, n) is:

$$H_T^{(k,n)} = H_0 + \sum_{j\neq k} c_j\lambda_j + (c_k + n\omega_0)\lambda_k$$

By making $n\omega_0$ the dominant term, the dynamics become primarily sensitive to c_k, this allows the NN to learn. For each of the $6 \times 10 = 60$ total experiments, we simulate the evolution $U_{k,n}(\tau) = \exp\Big(-iH_T^{(k,n)}\tau\Big)$ and compute a specific measurement, defined as

$$\arccos(|\langle 1| U_{k,n}(\tau) |1\rangle|)$$

The reason for this is explained in appendix A.

The fidelity will be calculated as

$$f_{ij} = \frac{1}{3}\operatorname{Tr}\Big(\langle i| U^\dagger U |j\rangle\Big)$$

To see whetter our method is good or not, we will use equation () to compare the real coefficients with the ones guessed by the NN's. So, first we get a set $\{c_i\}$, construct a H_{real} with this and a $H_{guessed}$ utilizing the guessed coefficients of our NN's. Then, we observe the quantity:

$$f_{11}(t) = \frac{1}{3}\operatorname{Tr}\Big(\langle 1| U_{guessed}^\dagger(t) U_{real}(t) |1\rangle\Big) \tag{1}$$

and, if $f_{11}(t) \approx 1$, then our approach is valid.

2.4 Neural Network Architecture and Training

We use a deep neural network (DNN) to solve this inverse problem: inferring the noise coefficients (outputs) from the simulated measurements (inputs).

Training data is generated by first sampling a set of six random noise coefficients c_k from a uniform distribution. Then, the 60 corresponding features are simulated as described in section 2.3. This (features, coefficients) pair forms one data point.

We trained one separate DNN for each of the six noise coefficients c_k. The 60 features serve as the input to each network, and each network is trained to output its corresponding single coefficient c_k. The combined set of six DNNs can then be used to predict the full noise Hamiltonian H_{int}. It is worth mentioning that the exact same data is used to train each coefficient.

To train our model, we will use MSE has loss, converting it in RMSE for analyzes.Formally,

$$\text{MSE} = \frac{1}{N}\sum_{i=1}^{N}(y_i - y_i')^2, \quad \text{RMSE} = \sqrt{\text{MSE}} = \sqrt{\frac{1}{N}\sum_{i=1}^{N}(y_i - y_i')^2}$$

where y_i are true values and y_i' are predicted values. Before going into the Network, we normalize data, setting its range from 0 to 1. With this, an RMSE of 0.01 means that the model's predictions are, on average, only about 1% away from the true values, an extremely small deviation.

3 Results

The Neural Networks were trained using a dataset of size 30000, following the protocol described is section 2. The training process was efficient, requiring a maximum of 400 epochs and a minimum of 109 to converge. The training history of each NN predicting each coefficient is shown below.

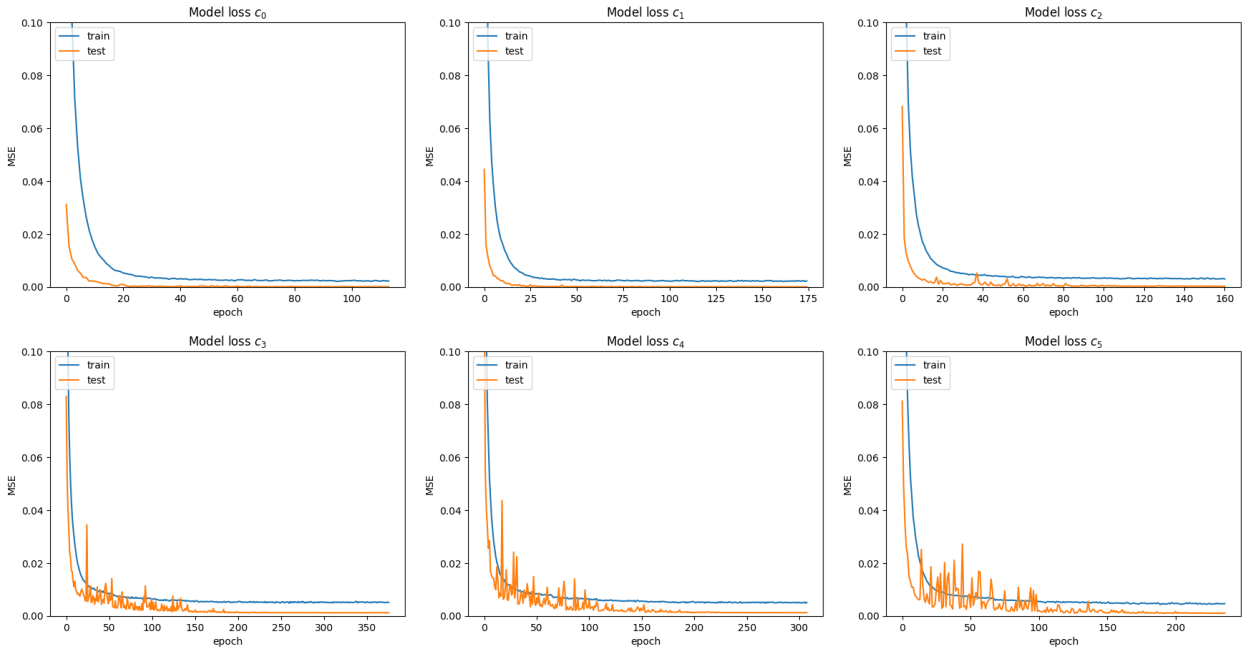

Figure 1: Model Loss

Important information about figure 1 is resumed in table below

Coefficient	MSE	RMSE	Epoch's
c_0	0.42×10^{-4}	0.0065	70
c_1	0.18×10^{-4}	0.0042	130
c_2	2.06×10^{-4}	0.0144	120
c_3	12×10^{-4}	0.0346	330
c_4	12×10^{-4}	0.0364	263
c_5	9.69×10^{-4}	0.0311	192

Table 1: Minha primeira tabela.

As expected (appendix A), the coefficients corresponding to the qubit subspace performed better than the rest, with a maximum RMSE of 1.14×10^{-2}, witch gives a deviation of only 1%. The other coefficients still performed well, with a deviation of 3%.

To validate our method's practical relevance, we tested its ability to reconstruct the noise Hamiltonian on a timescale relevant to real quantum gates. Following section 2.3, we simulated a real evolution U_{real} with a randomly chosen static noise Hamiltonian. We then uses our trained networks to predict the noise coefficients $\{c_k\}$ from simulated measurements. We then calculated the fidelity using equation (1) for fast (50ns) and slow (300ns) gates.

As shown in Figure 2, the fidelity comparing the real and guessed Hamiltonians matches closely over a 50 ns timescale.

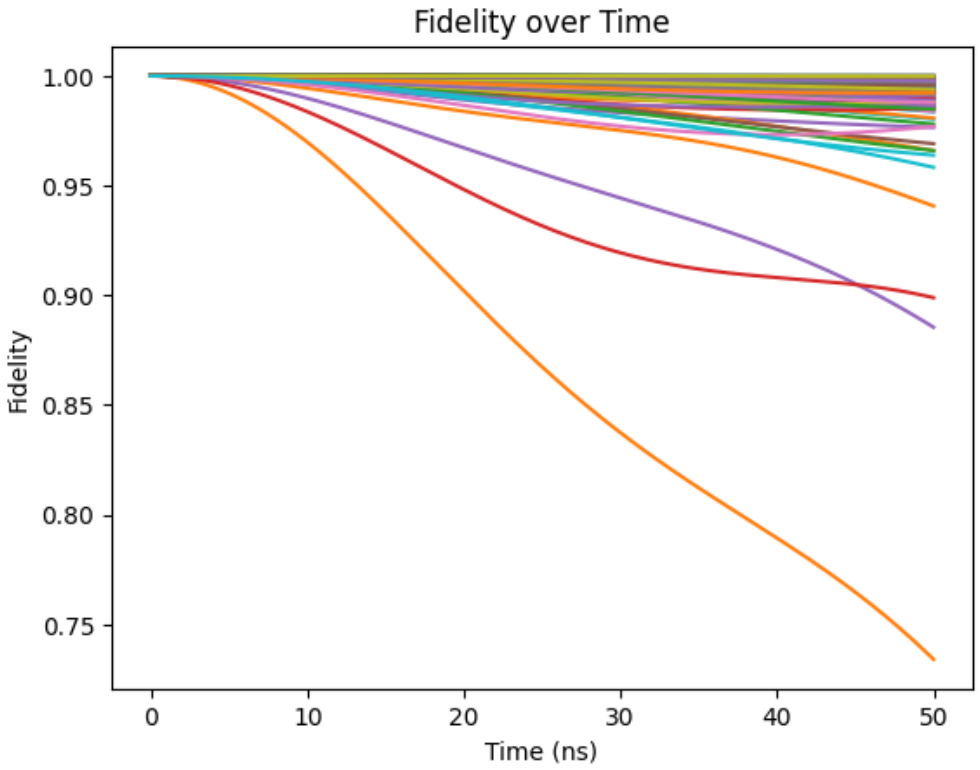

Figure 2: Fidelity over time for fast gates (50ns)

Samples	Mean	Standar deviation	75%	min
500	0.996	0.015	0.997	0.734

Table 2: Minha primeira tabela.

For 500 cases, we get some outliers, but considering a mean of 0.996 and Standard deviation of 0.015, we consider this a excellent result.

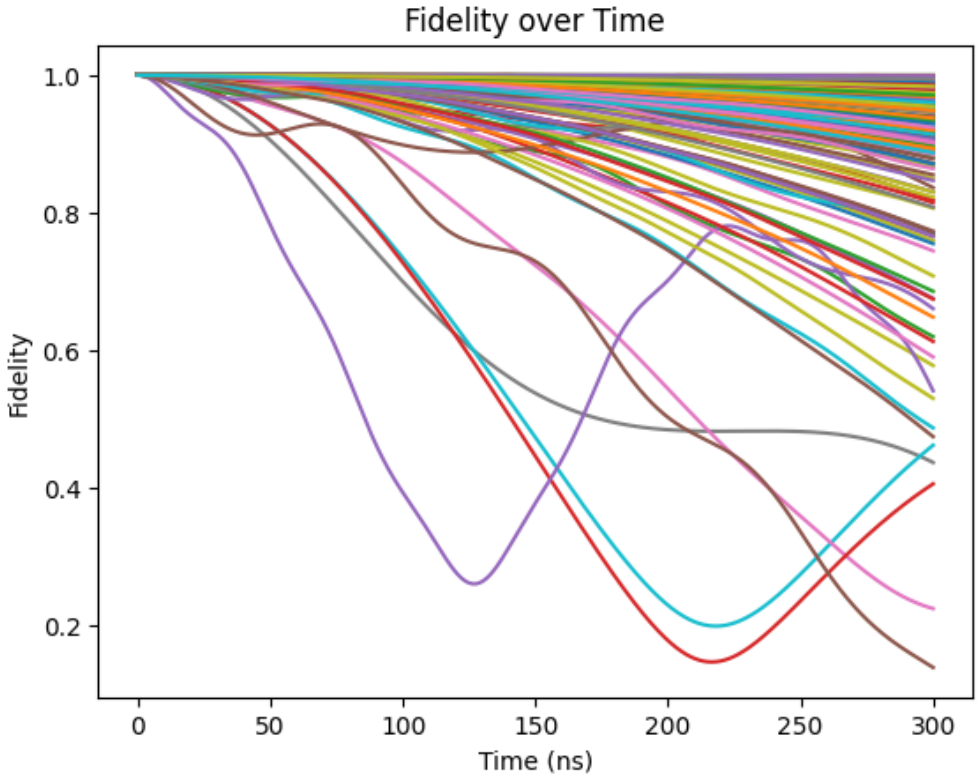

Figure 3: Fidelity over time for slower gates (300ns)

Samples	Mean	Standar deviation	75%	min
500	0.950	0.098	0.948	0.138

Table 3: Minha primeira tabela.

Now, for slower gates, results got worse. The number of outliers grew quite a lot, going below 0.7 in fidelity. Despite that, 75% of samples got a fidelity bigger then 0.948. With a mean of 0.95, our method is effective in most cases. It is worth remembering that the noise generated is 10 times stronger than normal and the coefficients are completely random, so we consider that this result still can get useful information about noise in the majority of cases.

4 Conclusion

In this work, we demonstrated a method to reconstruct an arbitrary static noise Hamiltonian in a qutrit system. The framework relies on a series of designed control pulses and a set of deep neural networks to

solve the inverse problem of characterization.

For the case of fast gate operations (50 ns), the trained network achieved a mean fidelity of 0.996, which is practically exact, with few outliers going below 0.950. Now, for slower gates operations (300 ns), there was a small decay of fidelity, with a mean of 0.950, but the number of outliers grew substantially, going below 0.8.

This level of precision is more than sufficient for accurately modeling noise on the timescale of quantum gate operations below 50ns. For times up to 300ns, we can't ensure the precision of our method, but in most cases, it can accurately model noise.

For future work, we plan to extend this method to handle non-static (time-dependent) noise, potentially by training the neural networks to predict a probability distribution for the noise coefficients rather than a single static value.

References

[1] FEYNMAN, R. P. Simulating physics with computers. *International Journal of Theoretical Physics*, v. 21, n. 6-7, p. 467-488, 1982. Disponível em: https://vql.cs.msu.ru/Feynman.pdf. [592, 593]

[2] GROVER, L. K. A fast quantum mechanical algorithm for database search. In: *Proceedings of STOC '96*. [S.l.: s.n.], 1996. p. 212-219. Disponível em: https://dl.acm.org/doi/10.1145/237814.237866. [594, 595]

[3] SHOR, P. W. Polynomial-time algorithms for prime factorization and discrete logarithms on a quantum computer. *SIAM Journal on Computing*, v. 26, n. 5, p. 1484-1509, 1997. Disponível em: https://epubs.siam.org/doi/10.1137/S0097539795293172. [596, 597]

[4] CAO, Y.; ROMERO, J. et al. Quantum chemistry in the age of quantum computing. *Chemical Reviews*, v. 119, n. 19, p. 10856-10915, 2019. Disponível em: https://pubs.acs.org/doi/10.1021/acs.chemrev.8b00803. [598, 599]

[5] MCARDLE, S. et al. Quantum computational chemistry. *Reviews of Modern Physics*, v. 92, n. 1, p. 015003, 2020. Disponível em: https://link.aps.org/doi/10.1103/RevModPhys.92.015003. [600, 601]

[6] CHOW, J. C. L. Quantum computing in medicine. *Medicina*, v. 12, n. 4, p. 67, 2024. Disponível em: https://pmc.ncbi.nlm.nih.gov/articles/PMC11586987/. [602, 603]

[7] PRESKILL, J. Quantum computing in the nisq era and beyond. *Quantum*, v. 2, p. 79, 2018. Disponível em: https://quantum-journal.org/papers/q-2018-08-06-79/. [608, 609]

[8] IBM Quantum. Technology and roadmap. 2025. Página institucional. Disponível em: https://www.ibm.com/quantum/technology. [612]

[9] Quantinuum. Quantinuum's H-Series hits 56 physical qubits that are all-to-all connected. 2024. Blog. Disponível em: https://www.quantinuum.com/blog/quantinuums-h-series-hits-56-physical-qubits-that-are-all-to-all-connected-and [613, 614, 615]

[10] AASEN, D. et al. Roadmap to fault tolerant quantum computation using topological qubit arrays. 2025. Disponível em: https://www.microsoft.com/en-us/research/publication/

roadmap-to-fault-tolerant-quantum-computation-using-topological-qubit-arrays/. [616, 617, 618]

[11] SETHARES, W. A.; COAUTHORS. Instead of 'supremacy' use 'quantum advantage. *Nature*, v. 576, p. 213, 2019. Disponível em: https://www.nature.com/articles/d41586-019-03781-0. [619, 620]

[12] David F. Wise, John J. L. Morton, and Siddharth Dhomkar. Using Deep Learning to Understand and Mitigate the Qubit Noise Environment. *PRX QUANTUM* 2, 010316 (2021). Disponível em: https://doi.org/10.1103/PRXQuantum.2.010316.

[13] The Royal Swedish Academy of Sciences. Scientific Background to the Nobel Prize in Physics 2025. 2025. Documento técnico. Discute CQED e o transmon como design insensível a ruído de carga. Disponível em: https://www.nobelprize.org/uploads/2025/10/advanced-physicsprize2025.pdf. [623, 624, 625]

[14] HYYPPÄ, E. et al. Reducing leakage of single-qubit gates for superconducting quantum processors using analytical control pulse envelopes. 2025. Disponível em: https://arxiv.org/abs/2402.17757.

[15] CHIARO, B.; ZHANG, Y. Active leakage cancellation in single qubit gates. 2025. Disponível em: https://arxiv.org/abs/2503.14731. [651]

[16] STRAUCH, F. W. Dephasing-induced leakage in multi-level superconducting quantum circuits. 2025. Disponível em: https://arxiv.org/abs/2501.17008.

[17] GOIPORIA, P. et al. Suppressing errors with dynamical decoupling using pulse control on Amazon Braket. 2022. Disponível em: https://aws.amazon.com/blogs/quantum-computing/suppressing-errors-with-dynamical-decoupling-using-pulse-control-on-amazon-bra [652, 653, 654, 655]

[18] CHATTERJEE, A. Quantum Error Correction For Dummies. 2023. Disponível em: https://arxiv.org/abs/2304.08678. [632]

[19] RAHMAN, A.; EGGER, D. J.; ARENZ, C. Learning How to Dynamically Decouple. 2024. Disponível em: https://arxiv.org/abs/2405.08689. [633]

[20] NAPOLITANO, R. d. J. et al. Protecting operations on qudits from noise by continuous dynamical decoupling. *Physical Review Research*, v. 3, n. 1, 2021. ISSN 2643-1564. Disponível em: http://dx.doi.org/10.1103/PhysRevResearch.3.013235.

[21] NIELSEN, M. A. Neural networks and deep learning. In: *Determination Press*, 2015. cap. 4.

[22] Schreier, J. A. et al. Suppressing charge noise decoherence in superconducting charge qubits. 2008. *Physical Review B*, 77(18), 180502(R). Disponível em: https://arxiv.org/abs/0712.3581

[23] Martinis, John M. et al. Decoherence in Josephson Qubits from Barrier Defects. 2005. *Physical Review Letters*, 95(21), 210503. Disponível em: https://arxiv.org/abs/cond-mat/0504552

[24] Arute, F. et al. Quantum supremacy using a programmable superconducting processor. 2019. *Nature*, 574(7779), 505-510. (arXiv: https://arxiv.org/abs/1910.11333)

[25] Barends, R. et al. A fast, low-leakage, high-fidelity two-qubit gate for a programmable superconducting quantum computer. 2019. Disponível em: https://arxiv.org/abs/1903.02492

[26] Ayral, T., Metelmann, A., Clerk, A. A. Microwave-activated gates between a fluxonium and a transmon qubit. 2022. Disponível em: https://arxiv.org/abs/2206.06203